Bull Math Biol (2014) 76:1218–1240
DOI 10.1007/s11538-014-9951-9

Society for Mathematical Biology

ORIGINAL ARTICLE

Bifurcation Analysis of Models with Uncertain Function Specification: How Should We Proceed?

M. W. Adamson · A. Yu. Morozov

Received: 22 October 2013 / Accepted: 13 March 2014 / Published online: 1 May 2014

Abstract When we investigate the bifurcation structure of models of natural phenomena, we usually assume that all model functions are mathematically specified and that the only existing uncertainty is with respect to the parameters of these functions. In this case, we can split the parameter space into domains corresponding to qualitatively similar dynamics, separated by bifurcation hypersurfaces. On the other hand, in the biological sciences, the exact shape of the model functions is often unknown, and only some qualitative properties of the functions can be specified: mathematically, we can consider that the unknown functions belong to a specific class of functions. However, the use of two different functions belonging to the same class can result in qualitatively different dynamical behaviour in the model and different types of bifurcation. In the literature, the conventional way to avoid such ambiguity is to narrow the class of unknown functions, which allows us to keep patterns of dynamical behaviour consistent for varying functions. The main shortcoming of this approach is that the restrictions on the model functions are often given by cumbersome expressions and are strictly model-dependent: biologically, they are meaningless. In this paper, we suggest a new framework (based on the ODE paradigm) which allows us to investigate deterministic biological models in which the mathematical formulation of some functions is unspecified except for some generic qualitative properties. We demonstrate that in such models, the conventional idea of revealing a concrete bifurcation structure becomes irrelevant: we can only describe bifurcations with a certain probability. We then propose a method to define the probability of a bifurcation taking place when there is uncertainty in the parameterisation in our model. As an illustrative example,

M. W. Adamson · A. Yu. Morozov (✉)
Department of Mathematics, University of Leicester, Leicester LE1 7RH, UK
e-mail: am379@le.ac.uk

A. Yu. Morozov
Shirshov Institute of Oceanology, Moscow, Russia

we consider a generic predator–prey model where the use of different parameterisations of the logistic-type prey growth function can result in different dynamics in terms of the type of the Hopf bifurcation through which the coexistence equilibrium loses stability. Using this system, we demonstrate a framework for evaluating the probability of having a supercritical or subcritical Hopf bifurcation.

Keywords Structural sensitivity · System stability · Uncertainty · Local bifurcation · Sensitivity analysis · Predator–prey model

1 Introduction

The conventional approach to investigating mean-field biological models consists in specifying an ODE system up to the choice of model parameters, and performing a detailed parametric analysis of this system to produce bifurcation diagrams. Provided that a particular choice of the constituent model functions is well justified, or that considering different mathematical parameterisations does not influence the general model behaviour, such an approach is valid. However, due to the high level of inaccuracy in biological data as well as dependence of biological phenomena on the time and space scales considered, it is generally impossible to derive an exact functional form to represent a given biological process (Morris 1990; Englund and Leonardsson 2008; Cordoleani et al. 2011). Furthermore, recent research has indicated that models can be sensitive to small changes in the parameterisation of model functions, a type of sensitivity known as 'structural sensitivity' (Myerscough et al. 1996; Wood and Thomas 1999; Fussmann and Blasius 2005; Cao et al. 2008; Cordoleani et al. 2011; Adamson and Morozov 2012, 2014). For this reason, we should aim to develop frameworks for bifurcation analysis by which the uncertainty in model specification is not ignored, but is instead carried through our analysis and reflected in some quantitative and qualitative description of the possible bifurcations which can potentially occur in the model.

A notable example in which the presence of structural sensitivity in biological models can lead to uncertainty in the model behaviour is found in the 'paradox of enrichment' in a Rosenzweig–MacArthur predator–prey model (Rosenzweig 1971). The precise value of the carrying capacity at which the interior equilibrium is destabilised via a Hopf bifurcation can be shown to strongly depend on the particular form of the Holling type II functional response used (Fussmann and Blasius 2005; Adamson and Morozov 2012). In this case, unless we make a particular choice of functional response, we can no longer talk about a 'concrete' bifurcation, at a particular value and the conventional approach of parametric analysis no longer makes sense. An alternative approach in this case could be to leave the functional response unspecified and consider a probabilistic bifurcation analysis in which a Hopf bifurcation is represented by a continuous change in the probability of observing an unstable equilibrium (Adamson and Morozov 2012).

In this paper, we attempt to make a first step towards constructing a bifurcation portrait of a biological ODE-based model in the case the constituent functions are

generally uncertain but belong to a known *class of functions* (Logistic growth functions or Holling type II functions for example). In this case, the given class of functions does not necessarily specify the bifurcation structure of the model completely: picking two different functions belonging to this class may result into two qualitatively different bifurcation portraits. Here, we propose a method for determining the probability of a Hopf bifurcation in such a model being supercritical or subcritical. As an illustrative example, we investigate the criticality of the Hopf bifurcation in a ratio-dependent predator–prey model with an unspecified prey growth function, but the same technique can be applied to a wide range of biological models with unspecified constituent functions.

Our illustrative example here is justified by the importance of predator–prey models with a ratio-dependent predator functional response, which have recently received a significant amount of attention. In such models, consumption of prey is a function of the ratio between the predator and the prey density, which is believed to be more ecologically relevant than the 'classical' prey-dependent response in many cases (Arditi and Ginzburg 1989; Arditi et al. 1991; Reeve 1997; Bishop et al. 2006). There has been a considerable amount of research into bifurcation analysis of ratio-dependent predator–prey models (Kuang and Beretta 1998; Berezovskaya et al. 2001; Hsu et al. 2001; Xiao and Ruan 2001; Li and Kuang 2007; Haque 2009; Sen et al. 2012 as well as many other publications). In particular, it has been rigorously proved that the stability loss in the case of the logistic growth function always takes place via a supercritical Hopf bifurcation with the appearance of a stable limit cycle, which signifies a non-catastrophic and reversible regime shift for the ecosystem. On the contrary, in the case where the prey growth rate is subject to an Allee effect (i.e. it increases at low population densities), it has been shown that the Hopf bifurcation in this system is actually subcritical (Sen et al. 2012, 2014), in which case the loss of stability of the coexistence equilibrium results in an eventual population collapse. However, all the above results were found for a *fixed* parameterisation of the growth term: it is not clear whether or not they are sensitive to the choice of this parameterisation.

Using our methods of sensitivity analysis, we firstly show that all the previous theoretical results in the literature on the behaviour of ratio-dependent predator-prey models lack generality. In particular, we show that for a slightly different parameterisation of the growth function—which we call 'generalised logistic growth'—the Hopf bifurcation can be subcritical, whereas for some different parameterisation of an Allee effect, the Hopf bifurcation can be supercritical. Further, we consider a general class of functions which contains an uncountable set of parametric families of prey growth functions of logistic type, and for the given class of functions, we determine how the probability of having a particular type of Hopf bifurcation in the model depends on the degree of closeness between functions in the class. We show that even for very close prey growth functions, there can be a large degree of uncertainty in the bifurcation structure of the model. Finally, we suggest a practical rule for concluding whether or not the uncertainty in the model functions results in uncertainty in the bifurcation portrait of the model, and whether or not it can therefore be analysed using the standard methods of bifurcation analysis.

2 Model Equations

We shall investigate the following ratio-dependent predator–prey model as considered in Berezovskaya et al. (2001), Sen et al. (2012) and a number of other works. For the sake of simplicity, we already consider the dimensionless form of the model:

$$\dot{x} = x\tilde{r}(x) - \nu\frac{xy}{x+y}, \tag{1}$$

$$\dot{y} = \mu\frac{xy}{x+y} - \gamma y, \tag{2}$$

where x is the prey density, y is the predator density, ν is the maximal predation rate, and μ is the maximal predator growth rate. The term $\frac{xy}{x+y}$ is the ratio-dependent functional response of the predator (Arditi and Ginzburg 1989; Arditi et al. 1991; Reeve 1997), and the unspecified function $\tilde{r}(x)$ is the growth rate of the prey, γ is the mortality rate of the predator.

Model (1)–(2) with the prey growth $\tilde{r}(x)$ given by the classic logistic growth function $r_1(x) = s(1-x)$ has been studied in a large number of papers in almost every possible detail (Freedman and Mathsen 1993; Jost et al. 1999; Kuang and Beretta 1998; Berezovskaya et al. 2001; Hsu et al. 2001; Xiao and Ruan 2001). In particular, it was shown that the system can have a unique interior equilibrium, signifying species coexistence, which can be either stable or unstable depending on parameters, with, the stability loss of this equilibrium taking place via a supercritical Hopf bifurcation—that is, a small stable limit cycle emerges as a result (Kuang and Beretta 1998). It has also been rigorously proved that in the case of a stable interior equilibrium, there can be no limit cycle in the system (Hsu et al. 2001; Xiao and Ruan 2001; Haque 2009). The complete set of bifurcation portraits of (1)–(2) with the logistic growth function $\tilde{r}(x)$ are provided in Berezovskaya et al. (2001).

In the case where the prey growth is subject to the Allee effect (i.e. the per capita growth rate is initially an increasing function) Sen et al. (2012) investigated the properties of the system for the parabolic parameterisation, $r_2(x) = s(1-x)(\beta - 1)$, which is the standard representation of the Allee effect used in the literature (Lewis and Kareiva 1993; Owen and Lewis 2001). It was found that in the case of the Allee effect, the stability loss of the coexistence equilibrium takes place only via a subcritical Hopf bifurcation: in this case, the unstable limit cycle surrounding the stable equilibrium disappears, and the trajectories will eventually go to the origin, which becomes the global attractor in this system (Sen et al. 2012). This supercritical Hopf bifurcation is observed both in the case of a weak and a strong Allee effect, i.e. for $-1 < \beta < 1$, but for $\beta < -1$, i.e. in the case the per capita growth function is always decreasing and can be considered as a generalised logistic function, the Hopf bifurcation becomes supercritical again, as in the classical case $r_1(x) = s(1-x)$. This property allows us to hypothesise that the results obtained for the classic logistic function should be robust.

Below we shall show that this optimistic hypothesis is actually wrong, and the results obtained earlier are in fact rather function-specific: the eventual type of Hopf bifurcation will strongly depend on the choice of function parameterisation. In this

paper, we mostly focus on the case of the logistic-like growth rate of the prey. However, similar techniques can be implemented in the case of an Allee effect in the prey growth as well (see Sect. 5).

In this paper, we shall consider the following general definition of the logistic growth function:

Definition 1 The prey growth is described by a logistic growth function in the case the per capita growth rate function $\tilde{r} : [0, x_{\max}] \to \mathbb{R}$ satisfies the two following properties:

(i) $\tilde{r}(0) > 0$,
(ii) $\tilde{r}'(x) < 0 \; \forall x \in [0, x_{\max}]$

This definition is a generalisation of the 'classical' logistic growth function based on common sense as well as some prior research (Gilpin and Ayala 1973; Sibly et al. 2005; Freckleton et al. 2006). Similarly, for the growth subjected to the Allee effect, we propose the following definition. Here, for the sake of simplicity, we consider that $x_{\max} = 1$.

Definition 2 The prey growth exhibits an Allee effect in the case where the per capita rate function $\tilde{r} : [0, x_{\max}] \to \mathbb{R}$ satisfies the three following properties. For some value $c \in (0, x_{\max})$ we have

(i) $\tilde{r}'(x) > 0 \; \forall x \in [0, c)$,
(ii) $\tilde{r}'(x) < 0 \; \forall x \in (c, x_{\max}]$,
(iii) $\tilde{r}(c) > 0$.

The above formulation is based on the ecological notion of the Allee effect (Hopf and Hopf 1985; Wang and Kot 2001; Berec et al. 2007).

3 Defining the Type of a Hopf Bifurcation for a General Function

We will be mostly interested in determining the type, or criticality, of Hopf bifurcation depending on the parameterisation of a model function. However, similar methods can potentially be used to address other kinds of bifurcation (see the Discussion).

Note that the influence of the criticality of a Hopf bifurcation is far more than a local matter: it has important implications for the global stability of an ecosystem. When a Hopf bifurcation is supercritical, the loss of the stability of an equilibrium is *non-catastrophic*, since for a limited parameter range trajectories are guaranteed to converge to the stable limit cycle which will be consequently formed in its vicinity. Provided the amplitude of this limit cycle is small, the ecosystem can still be considered to be stable, and moreover, if the bifurcation is reversed, the system will return to the original equilibrium. On the other hand, when a subcritical Hopf bifurcation takes place, an unstable limit cycle—which bounds the basin of attraction of the equilibrium—shrinks and disappears, and trajectories starting near to the equilibrium will leave its vicinity altogether. Therefore, the loss of stability is *catastrophic* and can have a fatal effect on the persistence of species in the ecosystem, as trajectories may well converge to an extinction state.

In order to investigate the Hopf bifurcation for a general per capita prey growth function $\tilde{r}(x)$, we can use the same approach as taken by Adamson and Morozov (2012, 2014). The first step of this approach consists of leaving the function in question unspecified, and introducing investigation parameters to represent values taken by the system in the vicinity of a given equilibrium. We can then investigate local system properties in terms of these parameters (see also the related frameworks of generalised modelling, Gross and Feudel 2006 and critical function analysis, Kisdi et al. 2013). From Eqs. (1)–(2), we can easily find equations for the densities of species at a non-trivial equilibrium:

$$y^* = \frac{\mu - \gamma}{\gamma} x^*, \tag{3}$$

$$\tilde{r}\left(x^*\right) = \frac{\nu}{\mu}\left(\mu - \gamma\right). \tag{4}$$

We shall treat one of the values x^* and y^* as an independent parameter of our investigation, since $\tilde{r}\left(x^*\right)$ is fixed due to the equilibrium condition (4). It is convenient to choose x^* as a parameter since it is the dependent variable of the unknown function $\tilde{r}(x)$.

Here, we shall consider the case that $\tilde{r}$ is a logistic function (see Definition 1). It is easy to see from Eq. (4) that if $\tilde{r}$ is monotonically decreasing, there is always a unique non-trivial equilibrium in the system. If we allow an Allee effect, the situation becomes somewhat more complicated, and the number of equilibria in the system will depend on how many inflection points the growth function takes. In this case, we should also investigate the number of equilibria using the approach outlined in Adamson and Morozov (2014).

In order to determine when a Hopf bifurcation takes place in the system we need to consider the Jacobian matrix of the system. The appropriate computation of the Jacobian matrix at the interior equilibrium gives the following (after some simplification):

$$A = \begin{pmatrix} x^*\tilde{r}'\left(x^*\right) + \frac{\nu\gamma(\mu-\gamma)}{\mu^2} & -\nu\frac{\gamma^2}{\mu^2} \\ \frac{(\mu-\gamma)^2}{\mu} & -\frac{\gamma}{\mu}\left(\mu-\gamma\right) \end{pmatrix}, \tag{5}$$

where $\tilde{r}'\left(x^*\right)$ can be considered as an independent parameter. The conditions for a Hopf bifurcation are that a pair of complex conjugate eigenvalues must cross the imaginary axis, which can be expressed in terms of the determinant and trace of the Jacobian as $Tr\left(A\right) = 0$ and $Det(A) > 0$ (together with the standard transversality condition,). From those conditions, we obtain after some simplification that at the Hopf bifurcation the value of $\tilde{r}'\left(x^*\right)$ is related to x^* as:

$$\tilde{r}'\left(x^*\right) = \frac{1}{x^*}\left[\frac{\gamma}{\mu^2}(\gamma-\mu)(\nu-\mu)\right], \tag{6}$$

provided that the condition $\nu > \mu$ is satisfied (note that we always require that $\gamma < \mu$ to guarantee the existence of the positive equilibrium).

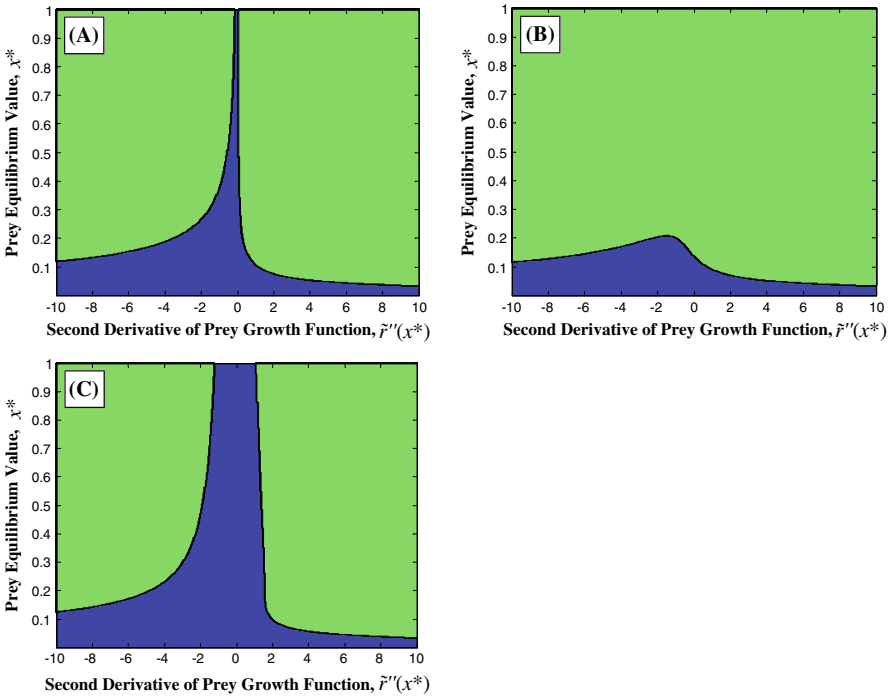

Fig. 1 Plots of the regions of sub- and super-criticality of the Hopf bifurcation in system (1)–(2) in the space of values of prey equilibrium density, x^*, and the second derivative of the prey growth function at this density, $\tilde{r}''(x^*)$, for three different values of the third derivative, $\tilde{r}'''(x^*)$. *Green regions* correspond to a subcritical Hopf bifurcation, while *blue regions* represent a supercritical Hopf bifurcation. **a** $\tilde{r}'''(x^*) = 0$. **b** $\tilde{r}'''(x^*) = 5$ is positive. **c** $\tilde{r}'''(x^*) = -10$ is negative. The model parameters used to construct the figures are $\nu = 2.7$; $\mu = 2$; $\gamma = 1.5$ (Color figure online)

A non-degenerate Hopf bifurcation can be of two types, supercritical—in which a stable limit cycle appears when the equilibrium is destabilised—or subcritical—in which an unstable limit cycle *disappears* when the equilibrium is destabilised. We can determine the criticality of a given Hopf bifurcation by computing the first Lyapunov number L_1 of the system at the Hopf bifurcation point: we have $L_1 < 0$ for a supercritical Hopf bifurcation and $L_1 > 0$ for a subcritical Hopf bifurcation. In a general planar system at a Hopf bifurcation, L_1 is given by an analytical expression (see "Appendix 1" for detail). However, computation of L_1 requires the coefficients of the third-order Taylor series expansion of the system about (x^*, y^*); thus, we need to specify values for the second and third derivatives of $\tilde{r}$ at the equilibrium, i.e. $\tilde{r}''(x^*)$ and $\tilde{r}'''(x^*)$. We shall consider these values as independent parameters of the investigation, along with the value of x^*. The criticality of a Hopf bifurcation in the system with a given prey growth function will be entirely determined by these three values alone.

A typical dependence of the criticality of the Hopf bifurcation in system (1)–(2) is shown in Fig. 1 for three fixed values of the third derivative, $\tilde{r}'''(x^*)$, the other model parameters being $\nu = 2.7$; $\mu = 2$; $\gamma = 1.5$. We see that in these cases there

are substantial regions of both supercritical and subcritical Hopf bifurcations, thus both supercritical and subcritical bifurcations are possible in the system with logistic growth. Note that the condition $\tilde{r}'(x^*) < 0$ is always satisfied for the given set of parameters [see expression (6)]. An important immediate conclusion is that previous well-known works on ratio-dependent predator–prey models (see citations in Sect. 2) predicting only a supercritical bifurcation may not be generic, but instead might be artefacts of the particular choice of parameterisation of $r(x)$. In particular, note that use of the standard logistic growth function with $r(x) = s(1 - x)$ immediately restricts us to the case $\tilde{r}''(x^*) = 0$, which, as can be seen from Fig. 1a, always lies in the supercritical Hopf bifurcation domain. Thus, the necessity of a supercritical Hopf bifurcation in the ratio-dependent model may only arise because the per capita growth rate is a linear function.

We should also mention that for a given parameterisation of $r(x)$, a Hopf bifurcation can take place strictly speaking only for a specific combination of ν, μ and γ: these parameters must be located on the Hopf bifurcation hypersurface. Indeed, the system of Eqs. (3), (4), and (6) with $r(x) = s(1 - x)$ has no solution for an arbitrary choice of ν, μ, γ. In particular, for the parameters chosen in Fig. 1a, no Hopf bifurcation is possible for the linear $r(x)$, and this fact provides a supplementary argument towards considering the general form of the growth rate function. On the other hand, direct computation confirms that the diagram remains similar (with $\tilde{r}''(x^*) = 0$ always being in the supercritical Hopf domain) even in the case where ν, μ, γ satisfy the Hopf bifurcation criteria for the linear $r(x)$.

A similar discrepancy with studies considering a particular parameterisation of the *Allee* effect in prey growth rate can be seen from Fig. 1. Indeed, for a generalised parameterisation of the Allee effect (see Definition 2), the stability loss of the equilibrium can take place both via a supercritical and a subcritical Hopf bifurcation (cf. Sen et al. 2012).

The results demonstrated in Fig. 1 have some importance consequences which extend well beyond the particular ratio-dependent model (1)–(2). How should we proceed in the case of such uncertainty? To somehow amend the situation and to go beyond well-known standard parameterisations, such as the logistic growth function $r(x) = s(1 - x)$ in (1)–(2), one can consider some other concrete parameterisations with the aim to conduct a thorough bifurcation analysis for each particular case by taking, for example, growth functions as $r(x) = s\left(1 - x^2\right)$, $r(x) = s(1 - \exp(x\alpha))$, the theta-logistic function (Gilpin and Ayala 1973), etc. The obvious drawback of this approach is that in each case, the investigation will be too specific, and we cannot, of course, 'cover' all possible parameterisations by picking up some arbitrary functions of our preference. Alternatively, we can utilise a more general approach by considering a generic function $r(x)$, for example, which satisfies Definition 1. In this case, we do not need to explore each concrete parameterisation separately, which is the main advantage of this method. However, to be able to construct a concrete bifurcation portrait in such a generic case, we need to restrict somehow the function $r(x)$, or else we may find ourselves in the situation where there are several different types of bifurcation structure (as in Fig. 1). One possible solution is to consider a narrow class of functions $r(x)$ that all provide equivalent bifurcation portraits. For instance, in system (1)–(2), a possible constraint on the function $r(x)$ could be that we consider

only those with a positive (or negative) Lyapunov exponent, L_1. However, to do this, we need to impose some analytical constraints on our functions, which are difficult to verify empirically and have no clear biological meaning. Moreover, such constraints are strictly model-dependent: in the case of a prey-dependent functional response, the condition $L_1 > 0$ will be given by a completely different equation. Thus, the above idea seems to lack any practicality.

In this paper, we suggest a novel combined approach to solving the problem raised above. We still consider a generic growth rate function $r(x)$ satisfying Definition 1, but since the use of different parameterisations can result in uncertainty in the bifurcation portrait (e.g. in different scenarios of Hopf bifurcation), we describe the resultant qualitative bifurcation outcome in terms of a probabilistic framework. Given a certain class of model functions, we aim to calculate the probability of the model having a particular type of bifurcation scenario. In the next section, we shall show how it can be possible in practice to evaluate the probability of having a supercritical Hopf bifurcation in model (1)–(2) for a generic class of functions $r(x)$ when a certain bifurcation parameter is varied.

4 Bifurcation Analysis Under Uncertainty in Model Functions

4.1 Determining Functional Neighbourhoods

We should stress that to proceed further with a bifurcation analysis of (1)–(2) with uncertain model functions, it is necessary to further restrict the class of functions $r(x)$ which are allowed. This need follows in part from the fact that the class of functions satisfying Definition 1 is still quite broad and can include some 'exotic' biologically meaningless parameterisations in a qualitative sense, but when we consider the empirical background of the model, there is also a need for a quantitative restriction of our functions. When we fit a parameterisation to a certain experimental or observation data set, we should take into account experimental error and therefore consider alternative parameterisations within a given distance from the fitted function to be also valid (e.g. Cordoleani et al. 2011), but if an alternative parameterisation passes too far away from the fitted function, and therefore the original data points, it should not be chosen as a viable alternative parameterisation. For this reason, we should only compare bifurcation scenarios for functions which are relatively close to each other across the whole admissible range of x.

There exist various ways of constructing a class of functions with close values across the entire range of x (here, we consider $x \in [0, 1]$). In this paper, we shall use the same idea as in Adamson and Morozov (2012) by introducing the *ε_Q-neighbourhood* of a certain base function. To do this, we first require that the unknown function belongs to some class of functions, Q, which satisfy the qualitative properties which are supported by theory or conjecture, e.g. a class of logistic functions as in Definition 1. We then make an initial concrete choice of the unknown model function—the 'base function' $r_0(x)$, which we should fit to data as far as possible. The ε_Q-neighbourhood of this function is then defined as the subset of functions in Q which are within a fixed distance of ε from the base function. For more details, refer to (Adamson and Morozov 2014).

The problem of working with neighbourhoods of functions is that they are infinite-dimensional, while certain critical model properties in the vicinity of an equilibrium are often entirely determined by local values of the function and some of its derivatives at the equilibrium (see Sect. 3). Therefore, it is important to relate the local function properties which are relatively easy to understand (see Fig. 1) and the global properties of the functions—their behaviour for any x. Our main idea is a projection of the infinite-dimensional function space into the finite-dimensional space of local function values: x^*, $\tilde{r}(x^*)$, $\tilde{r}'(x^*)$, $\tilde{r}''(x^*)$, and $\tilde{r}'''(x^*)$. Note that $\tilde{r}(x^*)$ is always fixed by (4), and in the case that there is a Hopf bifurcation $\tilde{r}'(x^*)$ will be fixed by (6), so in such cases we will only need to consider a 3D domain consisting of x^*, $\tilde{r}''(x^*)$ and $\tilde{r}'''(x^*)$. Due to the non-local restriction of functions $r(x)$, they should belong to the class Q and stay inside the ε_Q-neighbourhood of the base function $r_0(x)$—the values of x^*, $\tilde{r}'(x^*)$, $\tilde{r}''(x^*)$ and $\tilde{r}'''(x^*)$ cannot take arbitrary values, but will be located in the bounded domain. In this paper we consider the standard linear logistic function $r(x) = s(1 - x)$ as the base function (with $s = 1$). We also impose bounds on the second derivative: $-A < \tilde{r}''(x) < A \quad \forall x \in [0, x_{\max}]$, where A is a positive parameter. Finally, to simplify the analytical work, we consider that the actual function can be approximately considered as a cubic function—with constant third derivative $\tilde{r}'''(x^*)$—over a small interval about the equilibrium, $(x^* - w, x^* + w)$. In this case, given the values $\tilde{r}(x^*)$, $\tilde{r}'(x^*)$, $\tilde{r}''(x^*)$ and $\tilde{r}'''(x^*)$ and x^*, we can derive the necessary and sufficient conditions for the existence of a function of class Q in the ε_Q-neighbourhood of the linear base function taking these values (see "Appendix 2" for details).

In Fig. 2, we show examples of projections of the function space on the $x^* - \tilde{r}''(x^*)$ subspace for two different values of ν (n.b. actually, we show a *cross-section* of the 3-dimensional projection, since $\tilde{r}'''(x^*)$ is fixed in the given diagram). The domain corresponding to all the possible functions is bounded, since for the points located in the black domain there is no corresponding function in the ε_Q-neighbourhood. We

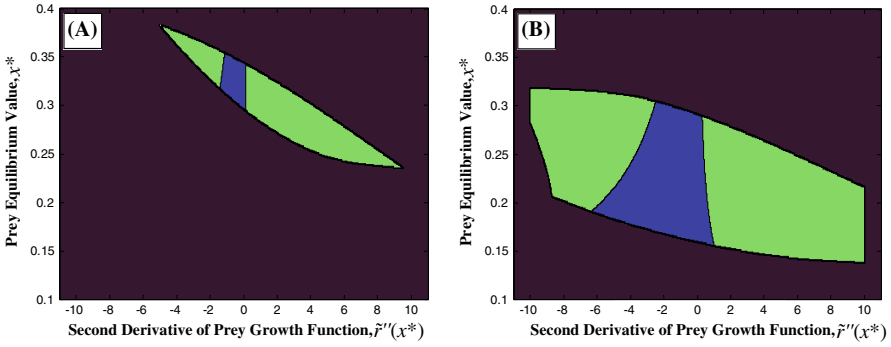

Fig. 2 Regions of the ε_Q-neighbourhood in $x^* - \tilde{r}''(x^*)$ space showing a supercritical and subcritical Hopf bifurcation for two given bifurcation values, ν^*. The *dark blue region* contains values outside the ε_Q-neighbourhood. Within the neighbourhood, *green* indicates the region in which the Hopf bifurcation will be supercritical, and *blue* indicates the regions in which it will be subcritical. The two bifurcation values are **a** $\nu^* = 2.7$. **b** $\nu^* = 3.1$.The other parameters are $\gamma = 1.5$; $\mu = 2$; $\varepsilon = 0.1$; $A = 10$; $w = 0.1$; $\tilde{r}'''\left(x^*\right) = 0$ (Color figure online)

can also see that the domain of possible functions still contains both supercritical and subcritical Hopf bifurcations scenarios. Note that the size of the ε_Q-neighbourhood depends on the model parameters as well as on ε or A. This follows from the fact that the values of $\tilde{r}(x^*)$ and $\tilde{r}'(x^*)$, which strongly influence the size of the ε_Q-neighbourhood, are not independent but are given by (4) and (6) and are therefore functions of ν, μ, and γ.

4.2 Constructing the Probability Density Function of a Hopf Bifurcation

Figures 1 and 2 showing the different domains of criticality are constructed under the assumption that we have a Hopf bifurcation for a given function at the parameter values ν, μ, γ. In general, this will not be the case for an arbitrary function of class Q in the ε_Q-neighbourhood of the base function. Therefore, to be able to evaluate the probability of having a particular type of Hopf bifurcation in the model, we first need to determine the probability of having a Hopf bifurcation at each parameter set in the first place.

The probability of having a Hopf bifurcation in the system within a given range of parameters (regardless of its criticality) will be determined by a certain probability density function (pdf). For the sake of simplicity, we fix two parameters (γ, μ) and consider the maximal attack rate, ν, as the sole bifurcation parameter in the system. For a given ν, we can plot the neighbourhood in the space of values x^* and $\tilde{r}'(x^*)$ corresponding to all functions in the ε_Q-neighbourhood, along with the Hopf bifurcation curve in this space (n.b. here, we consider the union of neighbourhoods for all $-A < \tilde{r}''(x^*) < A$ so that we obtain a two-dimensional plot, rather than considering the 3-dimensional space $x^* - \tilde{r}'(x^*) - \tilde{r}''(x^*)$). Examples of this neighbourhood for two different values of ν are shown in Fig. 3a, b, where we show the stability/instability of the stationary state for the given values of $x^*$and $\tilde{r}'(x^*)$, the value of $\tilde{r}(x^*)$ being fixed by (4).

If we denote the area of the region of stability by V_{stable}, and the total area of the neighbourhood by V, then, assuming that functions are uniformly distributed in all neighbourhoods, we can define the probability of the equilibrium being stable for a given parameter value ν as simply the relative area of the stability region:

$$P_\nu\,(\text{Stable}) = \frac{V_{\text{stable}}\,(\nu)}{V\,(\nu)}.$$

In Fig. 3c, we plot an example of how this probability changes with ν. One can see that the probability of having stability monotonically decreases from one to zero as the value of ν increases: the Hopf bifurcation curve moves from the upper left corner to the lower right corner. It is natural to define the probability density function (pdf) to have a Hopf bifurcation in the following way

$$p\left(\nu^* = \nu\right) := -\frac{d\,P_\nu\,(\text{Stable})}{d\nu}.$$

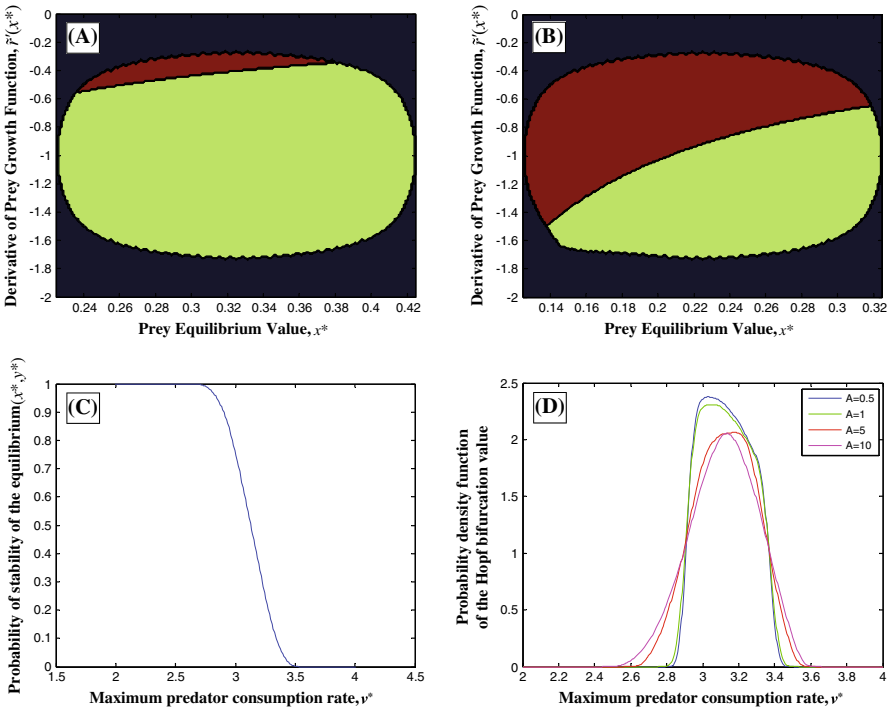

Fig. 3 Constructing the probability distribution of the bifurcation value, ν^*. **a**, **b** Regions of stability and instability in the ε_Q-neighbourhood of the base function $r(x) = 1 - x$ shown in $x^* - \tilde{r}'(x^*)$ space. *Dark blue regions* correspond to points outside the neighbourhood. Within the neighbourhood, *green regions* indicate stability of the interior equilibrium and *red regions* indicate it is unstable. The parameters are **a** $\nu = 2.7$; $\gamma = 1.5$; $\mu = 2$; $\varepsilon = 0.1$; $A = 10$; $w = 0.1$; $\tilde{r}'''(x^*) = 0$. **b** $\nu = 3.1$ all other parameters as in **a**. **c** Dependence of the stable proportion of the ε_Q-neighbourhood on the asymptotic predation rate, ν. All other parameters are the same as in **a**. **d** Probability distribution of the bifurcation value, ν^*. This is computed by taking the derivative of the stable proportion of the ε_Q-neighbourhood plotted in **c** with respect to ν. All other parameters are the same as in Fig. 2a (Color figure online)

The negative sign in this expression reflects the fact that the Hopf bifurcation is 'forward'—or destabilising with increasing ν. We should note that defining the pdf in this straightforward way is only valid if the bifurcation curve in Fig. 3a, b is shifted monotonically by a change in the parameter ν, as is the case here. Otherwise, we may have the situation where the bifurcation curve 'rotates', and the advance and retreat of the curve in different regions cancel each other out to some extent.

In the case that we have a precisely specified growth function $\tilde{r}(x)$ (including the parameter values), then Fig. 3c will be a step function, and $p(\nu^* = \nu)$ will be a delta function centred at the exact bifurcation value ν^*. To evaluate the probability of having a Hopf bifurcation in the range $[\nu_1, \nu_2]$, one needs to integrate the probability density function:

$$P(\nu \in [\nu_1, \nu_2]) = \int_{\nu_1}^{\nu_2} p(\nu^* = \nu) \mathrm{d}\nu \tag{7}$$

The range $[\nu_1, \nu_2]$ should be chosen so that a bifurcation definitely takes place within this interval, so the integral across the whole range of ν equals1.

Figure 3d shows the Hopf bifurcation pdf constructed numerically for several values of A, the maximal admissible curvature of $\tilde{r}$. We see that as we restrict A to lower values and therefore restrict ourselves to increasingly linear functions, the range of possible bifurcation values diminishes, although note that even when A is 0.5 there is still a wide range of potential bifurcation values.

4.3 Evaluating the Probability of Having a Supercritical Hopf Bifurcation

The next step in defining the probability of having a particular type of Hopf bifurcation is to derive the conditional probability of having a supercritical or subcritical bifurcation given that the bifurcation value is ν, P (Supercritical$|\nu^* = \nu$). We can compute P (Supercritical$|\nu^* = \nu$) in a similar way to how we found P_ν (Stable) in Sect. 4.2, i.e. by calculating the relative proportion of the area corresponding to the supercritical Hopf bifurcation in the total ε_Q-neighbourhood:

$$P\left(\text{Supercritical}|\nu^* = \nu\right) = \frac{V_{\text{supercritical}}(\nu)}{V(\nu)},$$

in the diagrams shown in Fig. 2. Note that, although in this paper we fix $\tilde{r}'''(x^*) = 0$ to simplify the diagrams, in practice there is no reason why we could not also vary this to gain a more complete analysis. Here, again we use the assumption that our functions are uniformly distributed in these neighbourhoods. In the Discussion, we suggest how this assumption can be relaxed.

In Fig. 4, we plot the distribution of the conditional probability P(Supercritical$|\nu^* = \nu$) for several values of maximum error, ε—recall that this term determines the width of the ε_Q-neighbourhood, or the maximum distance we allow $\tilde{r}$ to stray from the original logistic function while still being considered valid—and for several

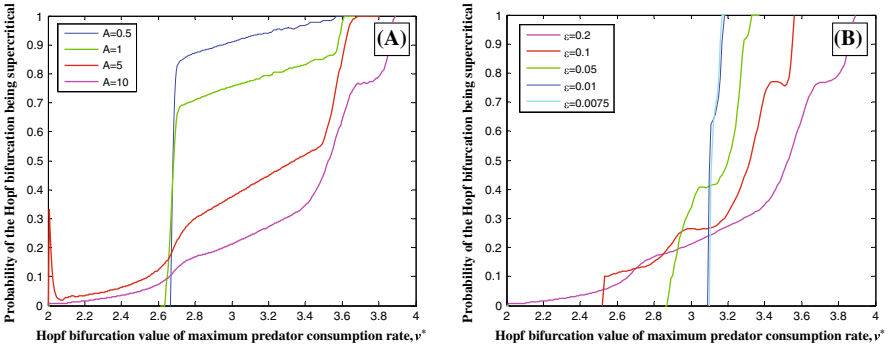

Fig. 4 Conditional probabilities of the Hopf bifurcation being supercritical given the bifurcation parameter is $\nu^* = \nu$. **a** Dependence on the maximum second derivative, A. All other parameters are the same as in Fig. 2a. **b** Dependence on the maximum error bound, ε. All other parameters are the same as in Fig. 2a (Color figure online)

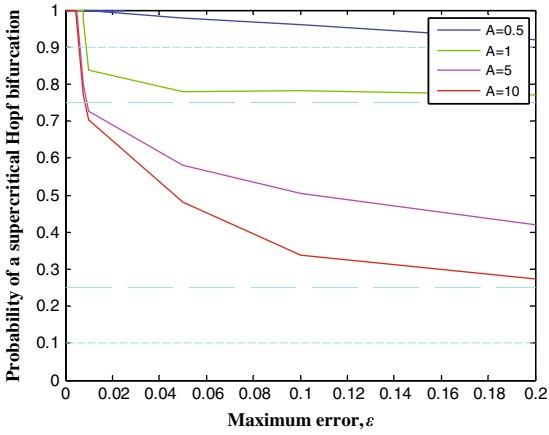

Fig. 5 Total probability of the Hopf bifurcation being supercritical as a function of ε, plotted for several values of A (Color figure online)

values of maximum curvature A—the largest absolute value of the second derivative of $\tilde{r}$, therefore giving a limit on how nonlinear $\tilde{r}$ can be. From Fig. 4a, we see that, as A is decreased and we restrict the second derivative more, $P\,(\text{Supercritical}|\nu^* = \nu)$ increases because we approach the case where $\tilde{r}$ is linear, in which case we will always have a supercritical bifurcation. In fact, when $A = 0.5$, we generally have $P\,(\text{Supercritical}|\nu^* = \nu) > 0.8$. Figure 4b shows a similar result when we decrease the maximal error in our function $\tilde{r}$, although the shift towards a higher likelihood of a supercritical bifurcation is less drastic that with a restriction to more linear functions.

Finally, once we have computed the pdf of the Hopf bifurcation value ν^* and the conditional probability of having a supercritical bifurcation given this bifurcation value, the overall probability of having a supercritical Hopf bifurcation in the system will be given through the total probability theorem:

$$P\,(\text{Supercritical}) := \int_{\nu_1}^{\nu_2} P\left(\text{Supercritical}|\nu^* = \nu\right) \cdot p\left(\nu^* = \nu\right) \mathrm{d}\nu, \tag{8}$$

where integration is done over all possible values of parameter ν for which a Hopf bifurcation of the interior equilibrium is possible.

In Fig. 5, we have plotted the total probability $P\,(\text{Supercritical})$ as a function of ε for several values of A using (8). Recall that the parameters have the following meaning: ε describes the accuracy of our data—the bigger the error terms, the larger ε should be; ε therefore determines the uncertainty in our model functions as a result of inaccuracies in data. A, on the other hand is the limit on the magnitude of the second derivative of the prey growth function, which gives us the estimate of how fast our per capita growth function can decease with x. Unlike ε, the choice of A is less straightforward and is more difficult to estimate from the data.

From Fig. 5, one can clearly see that in all cases the greater ε is, and therefore, the larger the error terms in our data (and the greater the uncertainty in our choice of functions), the probability of the Hopf bifurcation in the system being supercritical

decreases, and the more likely we should regard a subcritical bifurcation. As regards A, an increase—reflecting a modeller's choice to allow more nonlinearity in the growth functions considered, preferably based on empirical observation if possible—should cause us to expect a higher likelihood of the Hopf bifurcation being subcritical. The reason for this shift towards an increased likelihood of a subcritical bifurcation with an increase of ε and A is simply that linear functions always yield supercritical Hopf bifurcations since they restrict us to the line $\tilde{r}''(x^*) = 0$ in Fig. 1a, and so a relaxation of the linearity of our function—whether prompted by greater inaccuracy in our data or simply by modeller preference—increasingly allows the possibility of a subcritical Hopf bifurcation. Overall, in the case that ε is relatively large (and in biology it generally is), we should question whether our restrictions on the linearity of the growth term are valid, as an artificially low value of A can cause us to estimate an abnormally high probability of a supercritical Hopf bifurcation as a model artefact.

The figure also shows that for a gradual increase of the accuracy (i.e. a decrease in ε), the probability of having a supercritical Hopf bifurcation will eventually tend to 1, and we can be more or less certain about the type of bifurcation. If we allow the second derivative to vary within broad intervals, however, a high degree of uncertainty in terms of the type of bifurcation will remain until relatively small error terms (corresponding to a relative error of $\varepsilon \approx 2.5$–$5\,\%$). Note that typically the error ε is far greater than those values in any real biological experiments; thus, a high uncertainty in the bifurcation structure will be unavoidable if we allow a large curvature of the growth rate function. To reduce this uncertainty, we need to obtain some extra information regarding the bounds on the second derivative A (as well as the third derivative) of $r(x)$.

Another interesting result from Fig. 5 is what happens once the probability of the Hopf bifurcation being supercritical reaches 0.5. At this point, the chances of the bifurcation in the system being supercritical or subcritical are equally likely, so we have complete ambiguity with regards to which bifurcation type we should expect. Any further increase in ε from this will cause the probability of a supercritical bifurcation to fall further, and a subcritical bifurcation from this point will become increasingly more likely. This results in the almost paradoxical situation where greater uncertainty in our model functions should make us more, and not less confident in our model predictions.

Based on the probability plots shown in Fig. 5, we can classify the uncertainty in the bifurcation structure in model (1)–(2) by introducing a number of uncertainty levels. For instance, we can consider that in the case where $P\,(\text{Supercritical}) < 0.1$ or $P\,(\text{Supercritical}) > 0.9$, we do not have uncertainty in the bifurcation type and the model can be analysed using the standard methods of bifurcation analysis, despite the uncertainty in the model functions. In the case where we have $0.25 > P\,(\text{Supercritical}) > 0.1$ or $0.75 < P\,(\text{Supercritical}) < 0.9$, we can consider that a bifurcation of a certain type (i.e. either supercritical or subcritical) is to be *expected*; we can still use the deterministic framework, but we should always estimate the risk of overlooking the other bifurcation structure. For $0.75 > P\,(\text{Supercritical}) > 0.25$, we can say that we more or less have *complete uncertainty* regarding the bifurcation structure, and only probabilistic methods should be used in this case. We should stress

that the given levels of uncertainty are flexible and can be varied depending on the modelling task.

5 Discussion

Unlike models in physical sciences, where constituent functions in equations are unambiguously defined based on fundamental laws (e.g. Newtonian dynamics, quantum physics, etc), in biological sciences the choice of parameterisation of functions is often highly uncertain, and we need to take such uncertainty into account when constructing and analysing our models. In this paper, we have suggested a novel framework of how to include uncertainty in the parameterisation of model functions into the construction of corresponding bifurcation diagrams. The main idea is to allow a general class of model functions, which satisfies some general and biologically sound constraints, and consider the probability of having a particular bifurcation diagram. Thus, even in a purely deterministic dynamical system, uncertainty in the choice of functions can result in a probabilistic description in terms of what type of bifurcation diagram we should expect given a priori information about model functions. Here, we have provided a concrete example (based on a ratio-dependent model with unknown growth rate function) of how such a probabilistic analysis may be done: we evaluated the probability of having a supercritical Hopf bifurcation in the system where the uncertainty was only in the criticality of the bifurcation.

Our method is a more general alternative to other approaches such as fixing a few specific functional forms and proceeding as usual, then comparing the results, or combining them in a function $\alpha \cdot f(x) + (1-\alpha) \cdot g(x)$, and treating α as another parameter (e.g. Cordoleani et al. 2011). There are several existing frameworks which are related to our approach—indeed, there is a long history of research on biological models with unspecified functional forms going back as far as the pioneering work of Gause and Kolmogorov on general predator-prey systems (Gause 1934; Kolmogorov 1936). Firstly, the framework of generalised modelling and the analogous structural kinetic modelling (Gross et al. 2004; Gross and Feudel 2006; Steuer et al. 2006) shares with our method the use of unspecified functions which allow for a broad range of functional formulations to be considered, and the treatment of equilibrium values and the values of unknown functions/their derivatives as parameters in the Jacobian matrix of the system, although the elasticities of functions are normally considered instead of their derivatives for reasons of biological interpretability. A similar approach is taken in adaptive dynamics with critical function analysis (Mazancourt and Dieckmann 2004; Kisdi et al. 2013)—whereby evolutionary trade-off curves are left unspecified, and the type of a hypothetical evolutionarily singular strategy (in terms of evolutionary stability, convergence stability etc.) is determined using the local curvature of the trade-off function taken at the trait values taken by this strategy. Another framework for dealing with uncertainty in specific functional forms is to consider general canonical forms of equations, such as S-systems, for instance (Savageau and Voit 1987; Chou and Voit 2009), in which models are represented as systems of linear combinations of collective power law terms for given parameters, restricted to some (generally nonlinear) invariant manifold.

The work presented in this paper extends upon this body of work by constructing probability distributions in neighbourhoods on the space of local function values, in order to proceed beyond outlining what is possible and determine what behaviour is *probable* in a model. Notably, these neighbourhoods of local function values at an equilibrium are constructed based on the distance of functions from a certain base function across the *whole region* of the state variable—they may correspond, for instance, only to functions remaining within the red boundaries in Fig. 6. In this sense, the 'inputs' in our framework are not the local parameters corresponding to function values, elasticities etc. of the system at its equilibrium densities, as in generalised modelling, but global parameters such as the overall limit on the curvature of the function and the error term in data from which we then construct the relevant domain in the space of local parameters. Further, the neighbourhoods depend on global qualitative properties of the function and can therefore represent Holling type II functions, Logistic-type growth functions, etc. A further extension from generalised modelling is that we consider the criticality of a Hopf bifurcation here, which cannot be determined from the Jacobian alone.

One of the most surprising results of our investigation was that shown in Sect. 4.3—that an increase in the uncertainty in our model functions by increasing ε can result in us being more certain in the model bifurcation structure. Although we should note that in the investigation, whenever we observed this situation there was still a great deal of uncertainty, it may be possible to have a situation where the standard bifurcation investigation would be appropriate for large ε, but more accurate data should increase the uncertainty and cause us to switch to a probabilistic investigation. How can we justify this? It seems to suggest that in certain cases, less accurate data are in fact desirable. However, we should always aim to obtain data that are as accurate as possible as a priority—if we artificially increase the error terms considered, and so decrease the uncertainty in the bifurcation structure in this way, then this would poorly represent the amount of uncertainty that there truly is in the model bifurcation structure.

One of the main assumptions we have made in this paper is that the probability distribution in the space of local function values is uniform. This is, of course, far simpler than what we would expect in reality, and methods of constructing probability distributions should be improved. One approach is to use the 'functional density' approach outlined in Adamson and Morozov (2012). In this framework, the point $\left(x^*, \tilde{r}'\left(x^*\right), \tilde{r}''\left(x^*\right), \tilde{r}'''(x^*)\right)$ is weighted by the area of points in the ε_Q-neighbourhood that the graph of a function taking these values at x^* can pass through. This could be further improved by assigning weights to the points in graph space according to a normal distribution centred on the middle of the neighbourhood when we are calculating this area. Another approach is to derive a probability distribution of the local function values directly from the data points, but care must be taken to ensure that the resulting distribution is biologically relevant. Finally, we may aim to construct a more realistic distribution such as a Gaussian directly on the space of local values, modified such that our ε_Q-neighbourhood gives the 90 % confidence boundary, for instance. The trouble with this is that it is still arbitrary as to what the mean point is etc, and an incorrect assumption may lead to the resulting

distribution being even less realistic than the uniform distribution initially considered.

In this paper, we have solely considered the case where the growth term in model (1)–(2) is logistic and revealed that the standard result that the Hopf bifurcation in the system will always be supercritical in fact lacks generality when alternative functional forms are considered. The same question remains, however, with respect to the standard result that the Hopf bifurcation becomes subcritical when an Allee effect is introduced. Is this a general result, or simply an artefact of the particular functional forms of the growth rate used? Use of the standard Allee effect parameterisation $r(x) = (x - \beta)(1 - x)$ will automatically restrict us to the line $\tilde{r}''(x^*) = -2$ in Fig 1, for instance. Although this does not guarantee a subcritical Hopf bifurcation, certain resulting limitations on the equilibrium value x^* do, but it is easy to see that a choice of an alternative functional form may lift this restriction of $\tilde{r}''(x^*) = -2$ and potentially cause a supercritical bifurcation to become possible. Therefore, we can reasonably expect uncertainty in the criticality of the Hopf bifurcation which a standard bifurcation analysis will not be able to detect. An investigation using the framework outlined here would be desirable, although we note that the situation is slightly more complicated than the case with logistic growth. Consider Definition 2 as opposed to Definition 1: since the growth function is initially increasing, and then subsequently decreasing, it is possible that the number of interior equilibria can be either one or two depending on the particular functional form chosen. We should generally expect the first interior equilibrium to be a saddle point, however, and we can investigate the number of equilibria using the framework outlined in Adamson and Morozov (2014). Note that if we consider alternative formulations of the Allee effect, for instance, ones which exhibit a 'double' Allee effect in which the per capita growth function has two peaks (González-Olivares et al. 2011), the possible bifurcation portraits would be complicated significantly. Each extra peak allowed at the very least makes two additional interior equilibria possible.

Aside from a complete investigation into the Allee effect case, there are many other models which exhibit Hopf bifurcations, and it would be straightforward to implement a similar investigation on such systems to check the generality of their results. Furthermore, similar techniques can be applied to other local co-dimension one bifurcations, such as the saddle-node and transcritical bifurcations, for instance. We should also stress that there is no reason why we could not also consider co-dimension two bifurcations as well, such as Bogdanov–Takens bifurcations. Performing an analogous investigation for nonlocal bifurcations will be a lot more challenging, however. The approach here makes much use of the fact that local bifurcations conditions can be derived solely in terms of a finite number of terms of the Taylor series expansion of the system evaluated at an equilibrium, which is not the case for nonlocal bifurcations. This should be the next step if we wish to develop a framework for combining investigation of the various individual bifurcations into a complete probabilistic description of a system's bifurcation portrait. Finally, we can extend the method by considering several unknown functions in the model instead of a single one. This, however, can result in a dramatic increase in the overall complexity of the bifurca-

tion structure of the model through the appearance of multiple equilibria, limit cycles, etc.

Acknowledgments We highly appreciated S. V. Petrovskii (University of Leicester) for comments and suggestions.

Appendix 1: The First Lyapunov Exponent in a Planner System

The stability of a limit cycle is determined by its First Lyapunov number L_1. In the two-dimensional system

$$\begin{aligned}\dot{x} &= ax + by + f(x, y),\\ \dot{y} &= cx + dy + g(x, y)\end{aligned}$$

with $f(x, y) = a_{20}x^2 + a_{11}xy + a_{02}y^2 + a_{30}x^3 + a_{21}x^2y + a_{12}xy^2 + a_{03}y^3$, and $g(x, y) = b_{20}x^2 + b_{11}xy + b_{02}y^2 + b_{30}x^3 + b_{21}x^2y + b_{12}xy^2 + b_{03}y^3$, the first Lyapunov number is given by the following expression (Bautin and Leontovich 1976; Chow et al. 1994):

$$\begin{aligned}L_1 = -\frac{\pi}{4b\Delta^{\frac{3}{2}}}\Big\{\Big[&ac\left(a_{11}^2 + a_{11}b_{02} + a_{02}b_{11}\right) + ab\left(b_{11}^2 + b_{11}a_{20} + b_{20}a_{11}\right)\\ &+c^2\left(a_{11}a_{02} + 2a_{02}b_{02}\right) - 2ac\left(b_{02}^2 - a_{20}a_{02}\right) - 2ab\left(a_{20}^2 - b_{20}b_{02}\right)\\ &-b^2\left(2a_{20}b_{20} + b_{11}b_{20}\right) + \left(bc - 2a^2\right)\left(b_{11}b_{02} - a_{11}a_{20}\right)\Big]\\ &-\left(a^2 + bc\right)\left[3\left(cb_{03} - ba_{30}\right) + 2a\left(a_{21} + b_{12}\right) + \left(ca_{12} - bb_{21}\right)\right]\Big\},\end{aligned}$$

where Δ is the determinant of the Jacobian matrix.

In the case where the first Lyapunov number, evaluated at the equilibrium at the Hopf bifurcation point, is positive, then the resulting limit cycle will be stable, and the Hopf bifurcation is supercritical. If the first Lyapunov exponent is negative, the resulting limit cycle will be unstable and so the Hopf bifurcation is a subcritical one (Kuznetsov 2004).

Appendix 2: Deriving the Projection from Function Space to the Space of Local Values

Here, we derive and sketch a proof of the necessary and sufficient conditions for the existence of a function $\tilde{r}$ in the ε_Q-neighbourhood of the base function r taking the values x^*, $\tilde{r}(x^*)$, $\tilde{r}'(x^*)$, $\tilde{r}''(x^*)$ and $\tilde{r}'''(x^*)$.

For $\tilde{r}$ to remain within the ε_Q-neighbourhood, it must first satisfy:

$$\begin{aligned}&\tilde{r}(x) < r_{\varepsilon+}(x) = 1 + \varepsilon - x, \text{ and}\\ &\tilde{r}(x) > r_{\varepsilon-}(x) = 1 - \varepsilon - x.\end{aligned}$$

Essentially, this means that $\tilde{r}(x)$ must remain between the red bounds in Fig. 6 over the whole domain—it must remain within distance ε of the base function.

$\tilde{r}$ must also be in Q, so must further satisfy:

(i) $\tilde{r}'''(x) = \tilde{r}'''(x^*) \ \forall x \in (x^* - w, x^* + w)$,
(ii) $\left|\tilde{r}''(x)\right| < A \quad \forall x \in [0, x_{\max}]$,
(iii) $\tilde{r}'(x) < 0 \quad \forall x \in [0, x_{\max}]$,
(iv) $\tilde{r}(0) > 0$.

Condition i) tells us that across the interval $(x^* - w, x^* + w)$, $\tilde{r}$ is given by the cubic:

$$\tilde{r}(x) = \tilde{r}\left(x^*\right) + \tilde{r}'\left(x^*\right)\left(x - x^*\right) + \tilde{r}''\left(x^*\right)\left(x - x^*\right)^2 + \frac{\tilde{r}'''(x^*)}{6}\left(x - x^*\right)^3 \quad (9)$$

Therefore, an initial necessary condition for the existence of a valid function $\tilde{r}$ attaining the values x^*, $\tilde{r}(x^*)$, $\tilde{r}'(x^*)$, $\tilde{r}''(x^*)$ and $\tilde{r}'''(x^*)$ is that this cubic must stay between $r_{\varepsilon-}$ and $r_{\varepsilon+}$ over this interval. In addition, this cubic must always have a negative first derivative and not have a second derivative of magnitude greater than A. Furthermore, $\tilde{r}$ will be bounded above by the parabolas tangent to the above cubic at $x^* - w$ and $x^* + w$ with second derivative A, and will be bounded below by the tangent parabolas with second derivative $-A$. These are given by the blue curves in Fig. 6. Taking these upper and lower bounds over the intervals $[0, x^* - w)$ and $(x^* + w, x_{\max}]$, together with the fact that $\tilde{r}$ must equal the cubic (B1) over $(x^* - w, x^* + w)$, we can construct the following functions:

$$P_1(x) = \begin{cases} B + C\left(x - x^* + w\right) - \frac{A}{2}\left(x - x^* + w\right)^2 : & x \in [0, x^* - w) \\ \tilde{r}\left(x^*\right) + \tilde{r}'\left(x^*\right)\left(x - x^*\right) + \frac{\tilde{r}''(x^*)}{2}\left(x - x^*\right)^2 + \frac{\tilde{r}'''(x^*)}{6}\left(x - x^*\right)^3 : & x \in (x^* - w, x^* + w) \\ D + E\left(x - x^* - w\right) - \frac{A}{2}\left(x - x^* - w\right)^2 : & x \in (x^* + w, x_{\max}] \end{cases}$$

and

$$P_2(x) = \begin{cases} B + C\left(x - x^* + w\right) + \frac{A}{2}\left(x - x^* + w\right)^2 : & x \in [0, x^* - w) \\ \tilde{r}\left(x^*\right) + \tilde{r}'\left(x^*\right)\left(x - x^*\right) + \frac{\tilde{r}''(x^*)}{2}\left(x - x^*\right)^2 + \frac{\tilde{r}'''(x^*)}{6}\left(x - x^*\right)^3 : & x \in (x^* - w, x^* + w) \\ D + E\left(x - x^* - w\right) + \frac{A}{2}\left(x - x^* - w\right)^2 : & x \in (x^* + w, x_{\max}] \end{cases}$$

where:

$$B = \tilde{r}\left(x^*\right) - w\tilde{r}'\left(x^*\right) + \frac{w^2}{2}\tilde{r}''\left(x^*\right) - w^3\tilde{r}'''\left(x^*\right),$$

$$C = \tilde{r}'\left(x^*\right) - w\tilde{r}''\left(x^*\right) + \frac{w^2}{2}\tilde{r}'''\left(x^*\right),$$

$$D = \tilde{r}\left(x^*\right) + w\tilde{r}'\left(x^*\right) + \frac{w^2}{2}\tilde{r}''\left(x^*\right) + w^3\tilde{r}'''\left(x^*\right),$$

$$E = \tilde{r}'\left(x^*\right) + w\tilde{r}''\left(x^*\right) + \frac{w^2}{2}\tilde{r}'''\left(x^*\right).$$

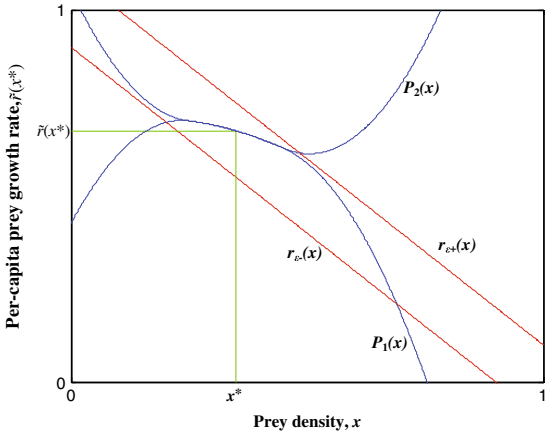

Fig. 6 Construction of the ε_Q-neighbourhood, as described in "Appendix 2". The *red lines* $r_{\varepsilon-}$ and $r_{\varepsilon+}$ denote points a distance ε from the (linear) base function. Any valid function must lie between these lines across the whole domain. The *blue curves* P_1 and P_2 represent the *lower* and *upper* bounds that necessarily hold for any function that belongs to the class Q. Valid functions must lie between these curves (and equal them across the domain $\left(x^* - w, x^* + w\right)$) (Color figure online)

For any function $\tilde{r} \in Q$, P_1 and P_2 necessarily form lower and upper bounds for $\tilde{r}$, since they are constructed as the extreme cases of functions in Q. So we have $P_1(x) \leq \tilde{r}(x) \leq P_2(x)\ \forall x \in [0, x_{\max}]$ (indeed, $\tilde{r}$, P_1 and P_2 coincide over the interval $(x^* - w, x^* + w)$), and therefore, the conditions:

$$\begin{aligned} P_1(x) &< r_{\varepsilon-}(x), \\ P_2(x) &< r_{\varepsilon+}(x), \\ P_1'(x) &< 0\ \forall x \in \left(x^* - w, x^* + w\right), \\ \left|P_1''(x)\right| &< A\ \forall x \in \left(x^* - w, x^* + w\right), \end{aligned}$$

are necessary (note: P_1, P_2 and $\tilde{r}$ coincide over the interval $(x^* - w, x^* + w)$ and so are interchangeable in the 3rd and 4th conditions). In terms of the figure, these conditions can be interpreted as requiring that the red upper and blue lower bounds clearly cannot cross.

It remains to be shown that they are sufficient. In order to prove this, it is enough to provide a method to construct a valid function $\tilde{r}$ which remains between $r_{\varepsilon-}$ and $r_{\varepsilon+}$ given only these conditions. We already have $\tilde{r}$ equal to P_1 and P_2 over $(x^* - w, x^* + w)$, so only need to construct $\tilde{r}$ over $[0, x^* - w)$ and $(x^* + w, x_{\max}]$. To do this, we can in fact use the exact same approach taken in Appendix 2 of Adamson and Morozov (2014).

References

Adamson, M. W., & Morozov, A Yu. (2012). When can we trust our model predictions? Unearthing structural sensitivity in biological systems. *Proc R Soc A Math Phys Eng Sci*, *469*, 20120500.

Adamson, M. W., & Morozov, A Yu. (2014). *Defining and detecting structural sensitivity in biological models: developing a new framework.*,. doi:10.1007/s00285-014-0753-3.

Arditi, R., & Ginzburg, L. R. (1989). Coupling in predator-prey dynamics: Ratio-dependence. *J Theor Biol*, *139*, 311–326.

Arditi, R., Ginzburg, L. R., & AkÿAkaya, H. R. (1991). Variation in plankton densities among lakes: a case for ratio-dependent models. *Am Nat*, *138*, 1287–1296.

Bautin, N., & Leontovich, Y. (1976). *Methods and procedures for the qualitative investigation of dynamical systems in a plane*. Moscow: Nauka.
Berezovskaya, F., Karev, G., & Arditi, R. (2001). Parametric analysis of the ratio-dependent predator-prey model. *J Math Biol*, *43*, 221–246.
Berec, L., Angulo, E., & Courchamp, F. (2007). Multiple Allee effects and population management. *Trends Ecol Evol*, *22*, 185–191.
Bishop, M. J., Kelaher, B. P., Smith, M., York, P. H., & Booth, D. J. (2006). Ratio-dependent response of a temperate Australia estuarine system to sustained nitrogen loading. *Oecologia*, *149*, 701–708.
Cao, J., Fussmann, G. F., & Ramsay, J. O. (2008). Estimating a predator-prey dynamical model with the parameter cascades method. *Biometrics*, *64*, 959–967.
Chou, I., & Voit, E. O. (2009). Recent developments in parameter estimation and structure identification of biochemical and genomic systems. *Math Biosci*, *219*, 57–83.
Chow S-N, Li C, Wang D (1994) Normal forms and bifurcation of planar vector fields. Cambridge University Press, Cambridge.
Cordoleani, F., Nerini, D., Gauduchon, M., Morozov, A., & Poggiale, J.-C. (2011). Structural sensitivity of biological models revisited. *J Theor Biol*, *283*, 82–91.
de Mazancourt, C., & Dieckmann, U. (2004). Trade-off geometries and frequency-dependent selection. *Am Nat*, *164*, 765–778.
Englund, G., & Leonardsson, K. (2008). Scaling up the functional response for spatially heterogeneous systems. *Ecol Lett*, *11*, 440–449.
Freckleton, R. P., Watkinson, A. R., Green, R. E., & Sutherland, W. J. (2006). Census error and the detection of density dependence. *J Anim Ecol*, *75*, 837–851.
Freedman, H. I., & Mathsen, R. M. (1993). Persistence in predator-prey systems with ratio-dependent predator influence. *Bull Math Biol*, *55*, 817–827.
Fussmann, G. F., & Blasius, B. (2005). Community response to enrichment is highly sensitive to model structure. *Biol Lett*, *1*, 9–12.
Gause, G. F. (1934). *The struggle for existence*. New York: Hafner Publishing Company.
Gilpin, M. E., & Ayala, F. J. (1973). Global models of growth and competition. *Proc Natl Acad Sci USA*, *70*, 3590–3593.
González-Olivares, E., González-Yañez, B., Lorca, J. M., Rojas-Palma, A., & Flores, J. D. (2011). Consequences of double Allee effect on the number of limit cycles in a predator-prey model. *Comput Math Appl*, *62*, 3449–3463.
Gross, T., Ebenhoh, W., & Feudel, U. (2004). Enrichment and food-chain stability: The impact of different forms of predator-prey interaction. *J Theor Biol*, *227*, 349–358.
Gross, T., & Feudel, U. (2006). Generalized models as an universal approach to the analysis of nonlinear dynamical systems. *Phys Rev E*, *73*, 016205.
Haque, M. (2009). Ratio-dependent predator-prey models of interacting populations. *Bull Math Biol*, *71*, 430–452.
Hopf, F. A., & Hopf, F. W. (1985). The role of the Allee effect in species packing. *Theor Popul Biol*, *27*, 25–50.
Hsu, S.-B., Hwang, T.-W., & Kuang, Y. (2001). Global analysis of the Michaelis-Menten-type ratio-dependent predator-prey system. *J Math Biol*, *42*, 489–506.
Jost, C., Arino, O., & Arditi, R. (1999). About deterministic extinction in ratio-dependent predator-prey models. *Bull Math Biol*, *61*, 19–32.
Kuang, Y., & Beretta, E. (1998). Global qualitative analysis of a ratio-dependent predator-prey system. *J Math Biol*, *36*, 389–406.
Kisdi, E., Geritz, S. A. H., & Boldin, B. (2013). Evolution of pathogen virulence under selective predation: A construction method to find eco-evolutionary cycles. *J Theor Biol*,. doi:10.1016/j.jtbi.2013.05.023.
Kolmogorov, A. N. (1936). Sulla Teoria di Volterra della Lotta per l'Esistenza. *Giornale Instituto Italiani Attuari*, *7*, 74–80.
Kuznetsov, Y. A. (2004). *Elements of applied bifurcation theory*. New York: Springer.
Lewis, M. A., & Kareiva, P. (1993). Allee dynamics and the spread of invading organisms. *Theor Popul Biol*, *43*, 141–158.
Li, B., & Kuang, Y. (2007). Heteroclinic bifurcation in the Michaelis-Menten type ratio-dependent predator-prey system. *SIAM J Appl Math*, *67*, 1453–1464.
Morris, W. F. (1990). Problems in detecting chaotic behavior in natural populations by fitting simple discrete models. *Ecology*, *71*, 1849–1862.

Myerscough, M. R., Darwen, M. J., & Hogarth, W. L. (1996). Stability, persistence and structural stability in a classical predator-prey model. *Ecol Model*, *89*, 31–42.

Owen, M. R., & Lewis, M. A. (2001). How predation can slow, stop or reverse a prey invasion. *Bull Math Biol*, *63*, 655–684.

Reeve, J. D. (1997). Predation and bark beetle dynamics. *Oecologia*, *112*, 48–54.

Rosenzweig, M. L. (1971). Paradox of enrichment: destabilization of exploitation ecosystems in ecological time. *Science*, *171*, 385–387.

Savageau, M. A., & Voit, E. O. (1987). Recasting nonlinear differential equations as S-systems: A canonical nonlinear form. *Math Biosci*, *87*, 83–115.

Sen, M., Banerjee, M., & Morozov, A. (2012). Bifurcation analysis of a ratio-dependent prey-predator model with the Allee effect. *Ecol Complex*, *11*, 12–27.

Sen, M., Banerjee, M., & Morozov, A. (2014). Stage-structured ratio-dependent predator-prey models revisited: when should the maturation lag result in systems' destabilization? *Ecol Complex, 19*, 23–34.

Sibly, R. M., Barker, D., Denham, M. C., Hone, J., & Pagel, M. (2005). On the regulation of populations of mammals, birds, fish, and insects. *Science*, *309*, 607–610.

Steuer, R., Gross, T., Selbig, J., & Blasius, B. (2006). Structural kinetic modeling of metabolic networks. *PNAS*, *103*, 11868–11873.

Wang, M. E., & Kot, M. (2001). Speeds of invasion in a model with strong or weak Allee effects. *Math Biosci*, *171*, 83–97.

Wood, S. N., & Thomas, M. B. (1999). Super-sensitivity to structure in biological models. *Proc R Soc Lond Ser B Biol Sci*, *266*, 565–570.

Xiao, D., & Ruan, S. (2001). Global dynamics of a ratio-dependent predator-prey system. *J Math Biol*, *43*, 268–290.